agriculture

MDPI

Article

Contact Parameter Calibration for Discrete Element Potato Minituber Seed Simulation

Kai Chen [1,2,3], Xiang Yin [1,2,3], Wenpeng Ma [1,2,3,*], Chengqian Jin [1,2,3,4] and Yangyang Liao [5]

[1] College of Agricultural Engineering and Food Science, Shandong University of Technology, Zibo 255049, China; xck817@163.com (K.C.); yinxiang@sdut.edu.cn (X.Y.); jinchengqian@caas.cn (C.J.)
[2] Institute of Modern Agricultural Equipment, Shandong University of Technology, Zibo 255049, China
[3] Shandong Key Laboratory of Intelligent Agricultural Technologies and Smart Agricultural Machinery Equipment for Field Crops, Zibo 255049, China
[4] Nanjing Institute of Agricultural Mechanization, Ministry of Agriculture and Rural Affairs, Nanjing 210014, China
[5] College of Engineering, China Agricultural University, Beijing 100083, China; 13210549525@163.com
* Correspondence: mawenpeng@sdut.edu.cn; Tel.: +86-134-3921-3276

Abstract: The discrete element method (DEM) has been widely applied as a vital auxiliary technique in the design and optimization processes of agricultural equipment, especially for simulating the behavior of granular materials. In this study, the focus is placed on accurately calibrating the simulation contact parameters necessary for the V7 potato minituber seed DEM simulation. Firstly, three mechanical tests are conducted, and through a combination of actual tests and simulation tests, the collision recovery coefficient between the seed and rubber material is determined to be 0.469, the static friction coefficient is 0.474, and the rolling friction coefficient is 0.0062. Subsequently, two repose angle tests are carried out by employing the box side plates lifting method and the cylinder lifting method. With the application of the response surface method and a search algorithm based on Matlab 2019, the optimal combination of seed-to-seed contact parameters, namely, the collision recovery coefficient, static friction coefficient, and rolling friction coefficient, is obtained, which are 0.500, 0.476, and 0.043, respectively. Finally, the calibration results are verified by a seed-falling device that combines collisions and accumulation, and it is shown that the relative error between the simulation result and the actual result in the verification test is small. Thus, the calibration results can provide assistance for the design and optimization of the potato minituber seed planter.

Keywords: potato minituber; discrete element; EDEM; repose angle; parameter calibration

Citation: Chen, K.; Yin, X.; Ma, W.; Jin, C.; Liao, Y. Contact Parameter Calibration for Discrete Element Potato Minituber Seed Simulation. *Agriculture* **2024**, *14*, 2298. https://doi.org/10.3390/agriculture14122298

Academic Editor: Simone Bergonzoli

Received: 19 November 2024
Revised: 9 December 2024
Accepted: 12 December 2024
Published: 14 December 2024

1. Introduction

Potato minituber is the original seed for propagating virus-free seed potato. It is of good quality and can significantly increase the potato yield per acre [1,2]. An efficient and low-damage potato minituber seeding device can effectively improve planting efficiency and reduce the use of labor. Discrete element method (DEM) is an effective numerical method for simulating the behavior of granular materials, and it is widely used in the design and research of agricultural equipment [3–6]. DEM can be used for the accurate simulation of the movement, collision, and interaction between potato minituber seeds, through which the complex phenomena of seed flow, mixing, and crushing during the seeding process can be accurately simulated as well, with a deeper understanding of these phenomena being enabled. Ultimately, this will optimize the mechanical structure, improve seeding efficiency and decrease seeding loss rate.

The calibration of contact parameters in simulation is the basis for the application of DEM. The validity of the simulation results will be directly affected by the accuracy of the calibration of the simulation contact parameters. Many scholars have calibrated the simulated contact parameters for various seeds or granular bodies, including cyperus esculentus seeds [7], kale root stubble [8], soil [9], morchella seed [10], and lily bulb [11].

Rao et al. [12] and Li et al. [13] determined the contact parameters between seed and contact material through three mechanical tests for rapeseed and mustard seed, respectively. Jin et al. [14] and Zhang et al. [15] used simulation tests to approximate the actual test method to obtain the contact parameters between the seed-contact material for maize seeds and green bean seeds based on three types of mechanical tests, making the calibration results closer to reality.

For the calibration of seed-to-seed contact parameters, it is not convenient to obtain them directly through tests, but they can be indirectly obtained through repose angle tests. The relative error between actual repose angle tests and simulation repose angle tests can be calculated, and the mathematical relationship between the simulated contact parameters and relative error can be established using the response surface method. This can indirectly obtain a set of optimal seed-to-seed contact parameter combinations [16–19]. Genetic algorithms (GA) can be used to search for the optimal seed-to-seed contact parameter combination. Li et al. [20] calibrated the parameters of silage through the optimized GA. GA have been widely used in many fields, including combinatorial optimization and scheduling problems, and have unique advantages in solving complex problems, such as global search ability, robustness, and parallelism [21–23].

Currently, most scholars in the study of seed-to-seed parameter calibration often use a single test device to obtain the angle of inclination. However, a single test device may not be able to better reflect the influence of seed-to-seed contact parameters on the angle of inclination, thereby reducing the accuracy of calibration. In this paper, the angle of inclination test method combining box lifting and cylinder lifting is adopted to balance the calibration error brought about by the test method, thereby improving the accuracy and rationality of the calibration results. At the same time, due to the thin skin of the potato minituber and its susceptibility to damage, the design of the seeding device adopts soft and smooth rubber materials to effectively reduce seed damage. However, there are still few studies on the parameter calibration between potato minituber seeds and rubber materials.

In the process of verifying the accuracy of the calibration results, most studies use a single repose angle test to compare the error between the simulation test and the actual test to verify the accuracy of the calibration results, such as the repose angle test of the cylinder lifting method [24–26]. However, this verification method mainly reflects the accuracy of seed-to-seed contact parameters and cannot effectively reflect the accuracy of seed–material contact parameters. This paper proposes a collision and accumulation combined verification device that can more comprehensively verify the accuracy of the calibration results and also provides a reference for the calibration of other granular body simulation contact parameters.

2. Materials and Methods

2.1. Intrinsic Parameter Determination and Model Establishment

2.1.1. Triaxial Size and Density of Seeds

The research object of this paper is the potato minituber seeds of the V7 variety (Zhangjiakou Academy of Agricultural Sciences, Zhangjiakou, China). This variety has a high yield, strong disease resistance, and a relatively wide planting area. In this paper, 200 seed samples were randomly selected to measure some of their intrinsic parameters. It was found through measurement that the size of the potato minituber of this variety is relatively uniform. The shape is mainly ellipsoidal, and a small part is spherical, with a ratio of approximately 4:1. The three-axis dimensions of the two shapes were measured separately by vernier calipers (Greenery Tools Co., Yantai, China). The average length (L), width (W), and thickness (T) of the ellipsoidal potato minituber were measured to be 18.2 mm, 11.9 mm, and 12.4 mm, respectively, and the average diameter of the spherical potato minituber was 11.6 mm. The triaxial dimensions of the potato minituber seed are shown in Figure 1.

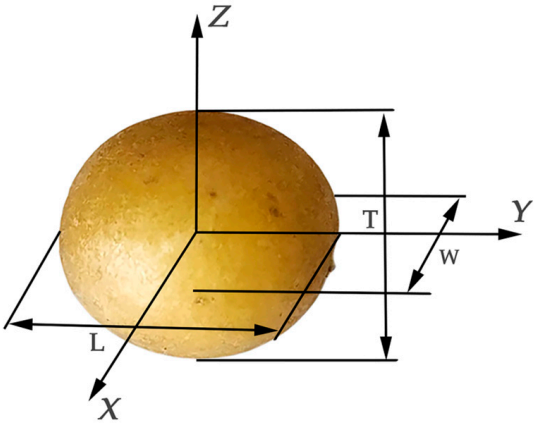

Figure 1. Potato minituber seed triaxial size.

The density of the seeds was measured by the water displacement method and was found to be 1012 kg/m^3, and the thousand-grain weight of the seeds was 1123.6 g.

2.1.2. Elastic Modulus and Poisson's Ratio

When conducting discrete element simulation, physical parameters such as the elastic modulus and Poisson's ratio of particles need to be input in the EDEM 2022 software. Compression tests using an Instron material testing machine and corresponding calculation equations can be employed to obtain the elastic modulus and Poisson's ratio of the seeds [27–29]. The potato minituber seeds are placed on the compression platform, and the pressure head applies pressure in the axial direction (thickness direction) of the seeds at a speed of 0.1 mm/s for 30 s before stopping (Figure 2). After the test is concluded, the axial load data of the material testing machine is read, and the lateral (width direction) and axial deformations of the potato minituber seeds are measured. Through Equations (1) and (2), it can be calculated that the elastic modulus of the seeds is 2.1 MPa and the Poisson's ratio is 0.32.

$$E = \frac{\sigma_s}{\varepsilon} = \frac{F/S}{\Delta T/T} \tag{1}$$

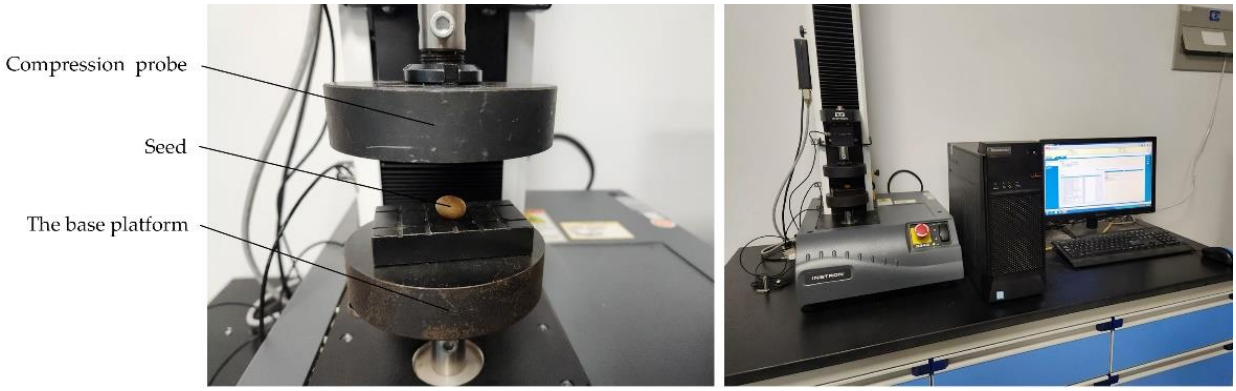

Figure 2. Miniature potato compression test.

In the equation, E represents the elastic modulus, MPa; σ_s represents the stress, MPa; ε represents the strain; F represents the axial load, N; S represents the contact cross-sectional area, mm^2; ΔT represents the thickness deformation of the seed after compression, mm; T represents the initial thickness before compression, mm.

$$\mu = \frac{|\varepsilon_w|}{|\varepsilon_t|} = \frac{\Delta W/W}{\Delta T/T} \tag{2}$$

In the equation, μ represents the Poisson's ratio; ε_w represents the lateral strain; ε_t represents the axial strain; ΔW represents the change in width after compression, mm; and W represents the initial width before compression, mm.

The high-elastic synthetic rubber produced by Hebei Jing dong Rubber Factory was selected as the rubber material in contact with the potato minituber in this paper. Its thickness is 4 mm, the Poisson's ratio is 0.47, and the elastic modulus is 1.2 MPa.

2.1.3. Establishment of Discrete Element Simulation Model

Based on the average three-axis dimensions and contours of the two seed shapes, 3D models were developed using Solidworks 2023, and these models were subsequently imported into EDEM 2022 software. According to parameters like the preset sphere radius range and the allowed degree of overlap, spheres were automatically filled into the space of the potato minituber. Multiple spheres were gradually combined to approximate the actual shape of the potato minituber, and appropriate filling effects were achieved by adjusting the parameters. The models are illustrated in Figure 3. For the simulation tests, a non-slip Hertz–Mindlin mechanical contact model was employed for analysis due to the smooth surface of the potato minituber seeds, which allows for negligible adhesion forces between them [30].

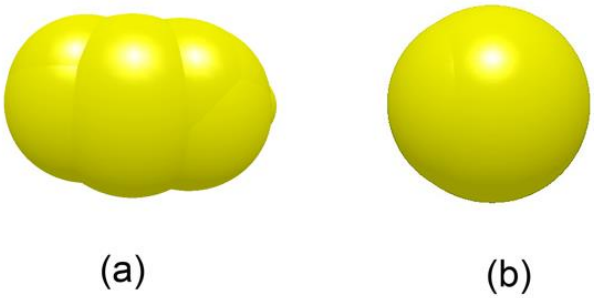

Figure 3. Potato minituber seed simulation model. (**a**) ellipsoidal model, (**b**) spherical model.

2.2. Calibration of Contact Parameters Between Seeds and Rubber Material

2.2.1. Calibration of Collision Recovery Coefficient Between Seed and Rubber Material

The coefficient of recovery is a fundamental physical parameter that quantifies the energy dissipation of an object during a collision. It plays a critical role in determining the post-collision motion state of particles and serves as an essential parameter in simulation processes. Through mechanical tests, the coefficient of recovery for particles can be measured, thereby providing a robust foundation for subsequent numerical simulations and theoretical analyses.

The coefficient of recovery (e_x) between two objects can be determined by calculating the ratio of the relative separation velocity following the collision to the relative approach velocity prior to the collision [31]. In this study, parameters were measured using a free-fall mechanical test (illustrated in Figure 4). Given that the potato minituber seeds were in motion while the rubber surface remained stationary, the coefficient of recovery is defined as the ratio of the instantaneous velocity (v_2) of the potato minituber seeds after colliding with the rubber surface to their instantaneous velocity (v_1) before impact. The calculation equation is presented as follows:

$$e_x = \frac{v_2}{v_1} = \frac{\sqrt{2gh_{max}}}{\sqrt{2gh_0}} = \frac{\sqrt{h_{max}}}{\sqrt{h_0}} \quad (3)$$

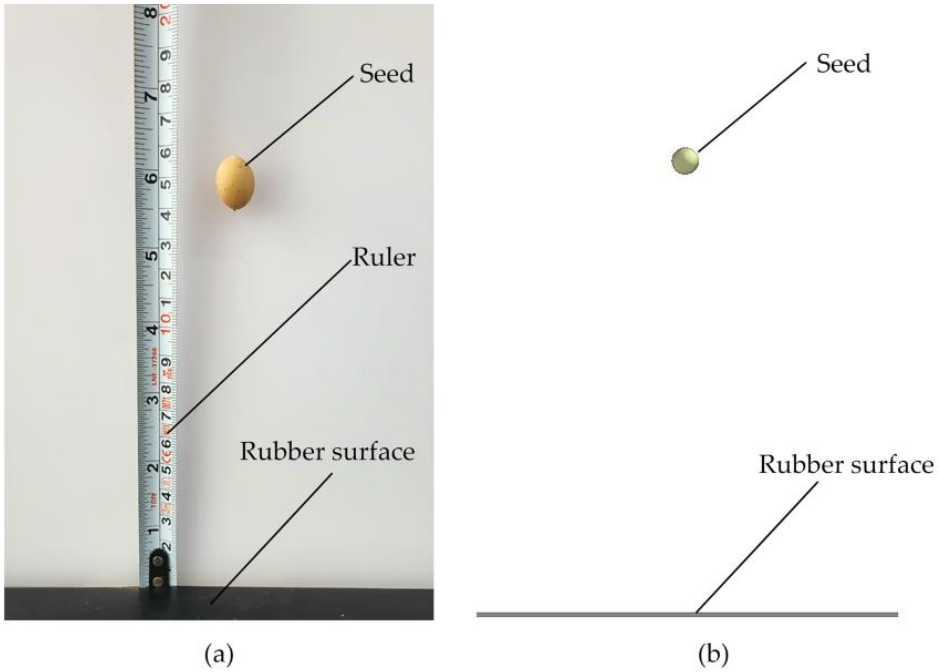

Figure 4. Potato minituber seed—rubber plate free fall test. (**a**) actual test, (**b**) simulation test.

In the equation, h_{max} represents the maximum rebound height of the seed, mm; h_0 indicates the initial height of the seed, mm.

Although the collision recovery coefficient can be initially calculated using Equation (3), the errors arising from various factors render it unsuitable for direct application in simulation tests, as this may compromise the accuracy of the results. Therefore, this study adopts a methodology that approximates actual tests through simulation to calibrate contact parameters.

Initially, the average maximum rebound height of seed particles was determined through actual free fall tests, and the collision recovery coefficient was subsequently calculated according to Equation (3). The parameter range for the simulation tests was established based on these computed values. Because the size difference between the spherical and ellipsoidal seeds in this variety is not significant, and it is easier to obtain a vertical upward bounce trajectory using spherical seeds for free fall tests, which makes height measurement easy. Therefore, spherical seeds were selected for both the actual tests and simulation tests. In Section 2.2.3, a similar reason was also chosen to use spherical seeds for the test.

In the actual free fall tests, seeds were released from an initial height of h_0 = 300 mm above a rubber surface, with h_{max} measured using high-speed imaging techniques. Given that potato minituber seeds possess an irregular circular shape, upward rebounds result in deviations; thus, 10 tests with minimal deviation were selected to obtain an average value. The test measured average h_{max} was found to be 73.4 mm. Utilizing Equation (3), the e_x value was computed as 0.495; consequently, a range of e_x values between 0.3 and 0.7—at intervals of 0.05—was designated for subsequent simulations.

A simulation environment mirroring the conditions of actual tests was constructed within EDEM software for conducting these simulations. Since free-fall tests involve negligible frictional forces, both static and rolling friction coefficients were set to zero in EDEM software settings. The e_x value was systematically varied during simulations to assess its impact on h_{max} values. The outcomes from nine free-fall simulation tests are summarized in Table 1.

Table 1. Results of free fall simulation test.

Test Number	Collision Recovery Coefficient	Maximum Rebound Height (mm)
1	0.30	20
2	0.35	39
3	0.40	58
4	0.45	70
5	0.50	84
6	0.55	96
7	0.60	119
8	0.65	141
9	0.70	169

The test results in Table 1 were plotted as a scatter diagram and a curve was fitted, as depicted in Figure 5. The fitting equation is

$$h_{max} = 274.46{e_x}^2 + 75.54e_x - 22.51 \quad (4)$$

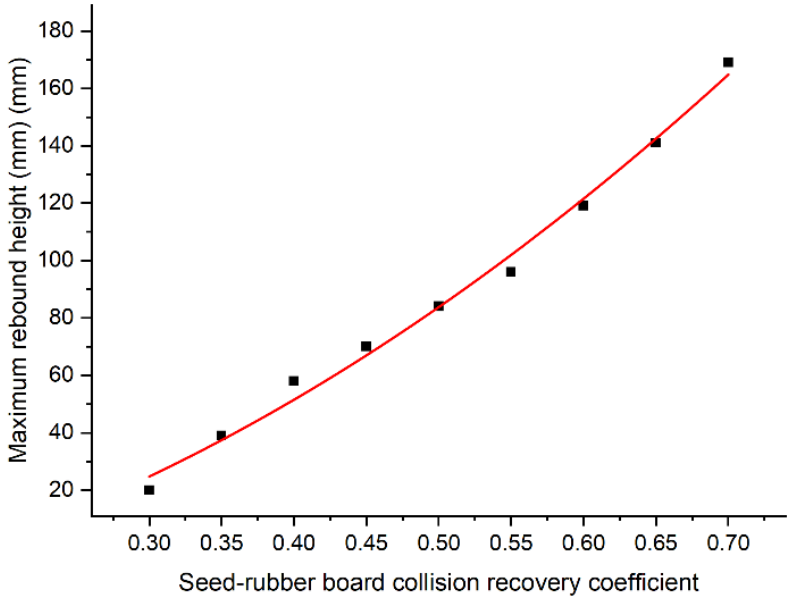

Figure 5. Collision recovery coefficient fits the curve.

The coefficient of determination R^2 for the fitting equation is 0.99, indicating a high level of reliability. Subsequently, by substituting the h_{max} of 73.4 mm obtained from actual tests into the aforementioned Equation (4), the e_x was determined to be 0.469.

This value was then reintroduced into EDEM for validation, yielding a measured maximum rebound height of 75.4 mm and a relative error of 2.7% compared to the actual measurement. The calculated e_x value of 0.495 obtained directly from the Equation (3) is also reintroduced into EDEM for verification, resulting in the maximum rebound height of 80.1 mm. The relative error between this value and the actual measured value is 9.1%. Therefore, 0.469 is selected as the calibration value.

2.2.2. Calibration of Static Friction Coefficient Between Seed and Rubber Material

Seed particles are likely to slide within seeding equipment; therefore, it is crucial to calibrate the static friction coefficient between the seeds and the rubber material. The static friction coefficient reflects the magnitude of frictional resistance encountered when seed particles slide, and it is influenced by both the roughness of the seed surface and that of the contact material, as well as by the contact area between them.

The static friction coefficient (μ_s) is defined as the ratio of the maximum static friction force (F_1) to the normal pressure (N). When a seed is positioned on an inclined plane and remains stationary without slipping, the component of its weight parallel to this incline (G_1) is less than the static friction force exerted by that incline on the seed particles. As one gradually increases the inclination angle, when a seed approaches a state where it is about to slip but has not yet, this static friction force reaches its maximum value and equals G_1. At this juncture, calculation of the static friction coefficient can be expressed as follows:

$$\mu_s = \frac{F_1}{N} = \frac{G_1}{N} = \frac{\text{mgsin}\,\alpha}{\text{mgcos}\,\alpha} = \tan\alpha \tag{5}$$

In the equation: The units of F_1, N, and G_1 are all N; α represents the inclination angle of the inclined plane, (°).

Consequently, in this paper, the inclined plane sliding method is employed to calibrate the static friction coefficient between the seeds and the rubber materials. The seeds are placed on the rubber bevel, and the inclination angle of the rubber bevel is gradually changed. The inclination angle is recorded when the seeds are on the verge of initiating sliding. Due to the oval shape of the seeds, they tend to roll rather than slide when placed on the inclined plane. Hence, four seeds are bonded together for measurement (as depicted in Figure 6).

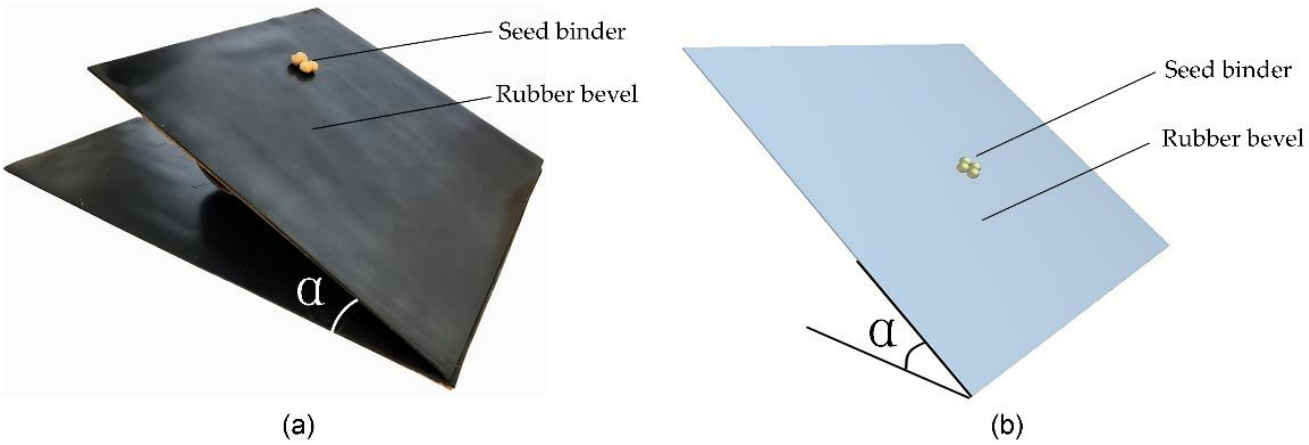

Figure 6. Slope sliding test. (**a**) actual test, (**b**) simulation test.

The test was repeated multiple times. A high-precision electronic angle gauge (with a measurement accuracy of ±0.01°, JINGYAN Co., DXL360S, Dongguan, China) was used to measure the angles. According to the Grubbs criterion, the data exceeding 3 times the standard deviation were removed, and then the average value of the 10 results was taken as the final result. The mean angle at which the seeds were on the verge of sliding was found to be 24.7°. Utilizing Equation (5), the static friction coefficient (μ_s) was determined to be 0.459. Consequently, for subsequent simulation tests, a μ_s range of 0.30 to 0.70 was selected, with an interval of 0.05.

A simulation model identical to that used in the actual test was established within the simulation software, as illustrated in Figure 6b. Under varying conditions of static friction coefficients, the inclination angle was incrementally increased, and the angle at which the seeds were about to slide was recorded accordingly. The collision recovery coefficient utilized in these simulations corresponded to a calibrated value of 0.469, while all other parameters were set to zero. Each group of simulation tests underwent ten repetitions, and average results were computed as presented in Table 2.

Table 2. Results of static friction simulation tests.

Test Number	Coefficient of Static Friction	Sliding Angle (°)
1	0.30	15.8
2	0.35	18.3
3	0.40	19.9
4	0.45	22.5
5	0.50	26.1
6	0.55	29.4
7	0.60	31.5
8	0.65	32.1
9	0.70	34.7

The test results were represented in a scatter plot (Figure 7), and a curve was fitted to the data. The fitting equation is as follows:

$$\alpha = -21.08{\mu_s}^2 + 70.12\mu_s - 3.85 \quad (6)$$

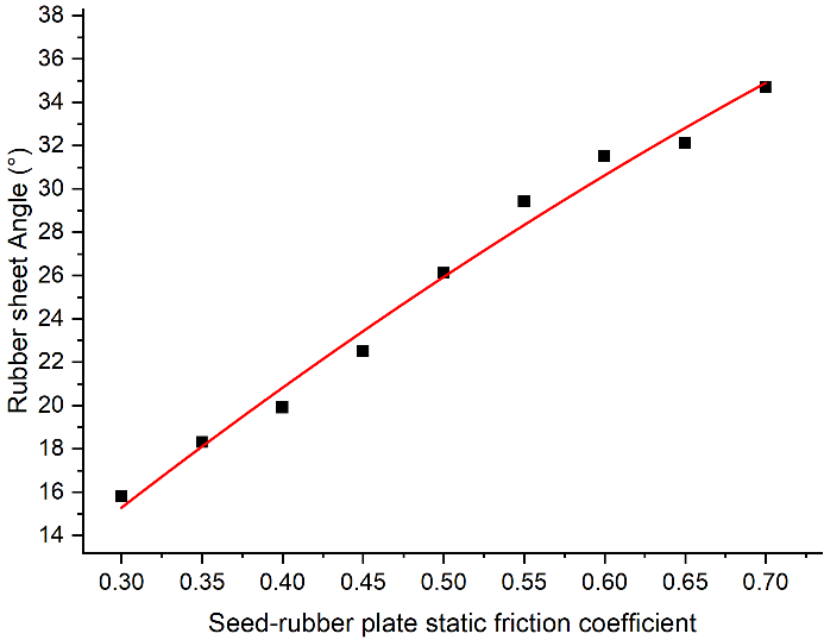

Figure 7. Static friction coefficient fitting curve.

The coefficient of determination R^2 for this fitting equation is 0.99, indicating a high degree of reliability. By substituting the measured angle—24.7° at which the seed began to slide during the actual test—into the Equation (6), μ_s was calculated to be 0.474.

This value was subsequently reintroduced into EDEM for verification purposes, yielding a measured inclination angle of 24.1°, resulting in a relative error of 2.4% compared to the actual value. The μ_s value of 0.459, which is directly calculated from Equation (5), is also reintroduced into EDEM for verification, resulting in an inclination angle of 23.4°. The relative error between this value and the actual measured value is 5.3%. Therefore, 0.474 is selected as the calibration value.

2.2.3. Calibration of Rolling Friction Coefficient Between Seed and Rubber Material

The potato minituber seeds exhibit an approximately spherical shape and possess a relatively smooth surface. Consequently, their rolling behavior in seeding devices is more pronounced compared to that of non-spherical seeds such as corn. The rolling friction coefficient (μ_r) is a physical parameter that quantifies the resistance encountered during the rolling motion of an object. It is defined as the ratio of the rolling friction force between

the surface of the rolling object and its contact surface to the gravitational force acting on the object, typically determined using the inclined plane rolling method.

The inclined plane dynamics test apparatus is illustrated in Figure 8 and comprises a rubber inclined plane connected to a horizontal rubber surface. When the seeds are released onto the inclined plane at a specified angle, they roll downwards and subsequently continue to roll along the horizontal surface until coming to rest. By measuring both the angle of inclination, seed release position, and distance traveled by each seed on this surface, one can calculate the rolling friction coefficient. For simplification purposes in analysis and computation, it is assumed that during their motion, only rolling friction influences these seeds while neglecting other factors such as air resistance. Thus, on this horizontal plane, seeds gradually come to rest due solely to rolling friction forces acting upon them. According to conservation of energy principles, during this process, any change in gravitational potential energy corresponds directly with work carried out against rolling resistance; thus leading us to derive our calculation equation:

$$\mu_r = \frac{\mathrm{mg}l_0 \sin\beta}{\mathrm{mg}(l_0 \cos\beta + l)} = \frac{l_0 \sin\beta}{l_0 \cos\beta + l} \tag{7}$$

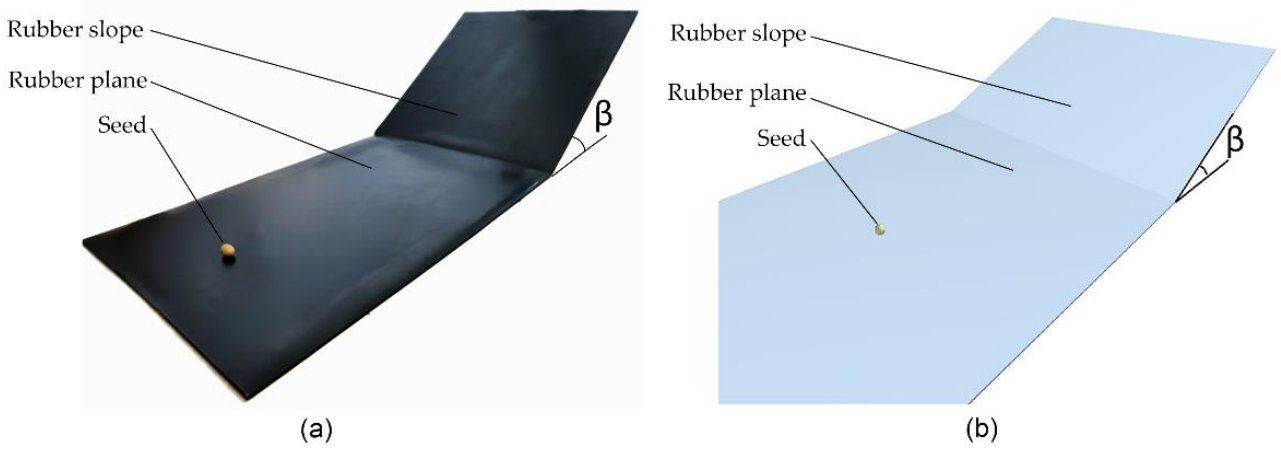

Figure 8. Inclined plane rolling test. (**a**) actual test, (**b**) simulation test.

In the equation, μ_r represents the value of the rolling friction coefficient; l_0 represents the distance from the release point of the seed on the rubber slope to the rubber plane, mm; l indicates the rolling distance of the seed on the rubber plane, mm; and β stands for the angle of the rubber slope, (°).

Given that the shape of the seeds is irregular, they do not maintain a linear motion during rolling. Hence, to ensure the accuracy of the test results, the rolling distance of the seeds should not be overly long. After several preliminary tests, the β was set at 8°, and l_0 was set at 30 mm. The test was replicated numerous times. The results of the 10 tests with relatively straight rolling trajectories were selected and averaged. Ultimately, the average rolling distance was measured to be 544 mm. μ_r was calculated based on Equation (7) and found to be 0.0071. Therefore, for the subsequent simulation tests, the range of the μ_r was chosen as 0.004 to 0.010, with an interval of 0.001.

In the simulation tests, the collision recovery coefficient and the static friction coefficient were respectively adopted as the calibrated values of 0.469 and 0.474. By continuously varying the μ_r value to conduct the simulation tests, the rolling distance l of the seeds on the rubber plane was recorded. Each group of simulation tests was replicated multiple times. Similarly, the results of the 10 tests with relatively straight rolling trajectories were selected and averaged. The results are presented in Table 3.

Table 3. Inclined plane rolling simulation test scheme and results.

Test Number	Coefficient of Rolling Friction	Rolling Distance (mm)
1	0.004	701
2	0.005	650
3	0.006	580
4	0.007	464
5	0.008	407
6	0.009	336
7	0.010	320

The simulation test results in Table 3 were plotted as a scatter diagram and fitted with a curve (Figure 9). The fitting equation is as follows:

$$l = 3{,}428{,}571.31\mu_r{}^2 - 117{,}428.56\mu_r + 1134.28 \quad (8)$$

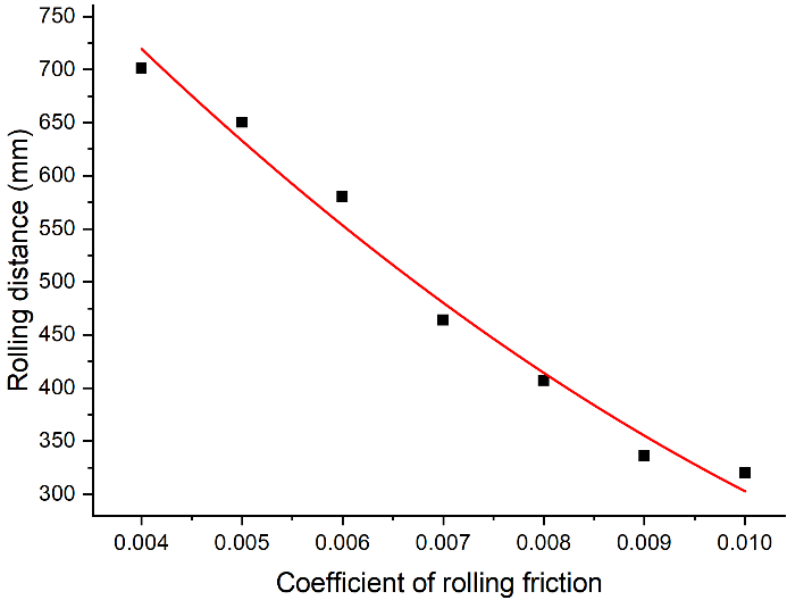

Figure 9. Rolling friction coefficient fitting curve.

The coefficient of determination R^2 of the fitted equation is 0.98, indicating a high level of reliability of the equation. By substituting the measured average horizontal rolling distance of 544 mm from the actual tests into the Equation (8), the μ_r between the potato minituber seeds and the rubber material was obtained as 0.0062.

This value was re-introduced into EDEM for verification, and the measured rolling distance was 523 mm. The relative error compared to the actual value was 3.8%. The μ_r value of 0.0071, which is directly calculated from Equation (7), is also reintroduced into EDEM for verification. The rolling distance was measured at 462 mm. The relative error between this value and the actual measured value is 15.1%. Therefore, 0.0062 is selected as the calibration value.

2.3. Calibration of Seed-to-Seed Contact Parameters

2.3.1. Repose Angle Test

Owing to the shape of the seeds, the aforementioned three calibration approaches are relatively more applicable for calibrating the parameters between seeds and planar contact materials, but not for the contact parameters between seeds. Hence, this paper employs the repose angle test to simultaneously calibrate the three seed-to-seed contact parameters. This paper will conduct both actual and simulation repose angle tests. Through the response

surface method and parameter optimization based on the genetic algorithm, the optimal combination of seed-to-seed contact parameters will eventually be obtained.

To minimize the calibration error resulting from the test approach as much as possible, this paper will adopt two types of repose angle test methods—the box side plates lifting method and the cylinder lifting method—for conducting the repose angle tests. Both test devices are assembled from acrylic panels. The test apparatus of the box side plates lifting method consists of two fixed side plates (length 150 mm, width 100 mm), two liftable side plates (length 150 mm, width 100 mm) and a square bottom trough (length 200 mm, width 100 mm, depth 12 mm), as shown in Figure 10a. The test devices of the cylinder lifting method consist of a liftable cylinder (diameter 80 mm, length 200 mm) and a circular bottom trough (diameter 150 mm, depth 20 mm), as shown in Figure 10b.

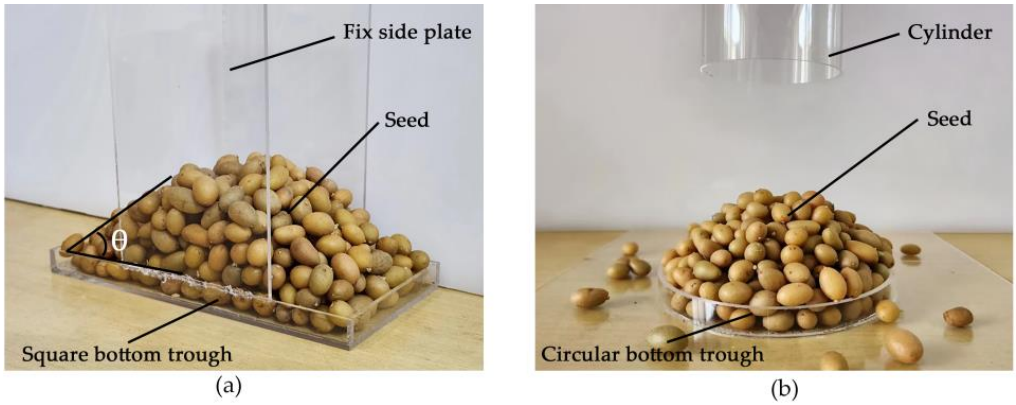

Figure 10. Repose angle test device. (**a**) box side plates lifting method, (**b**) cylinder lifting method.

Using a concave bottom instead of a flat surface to form the repose angle can reduce the calibration error caused by seed rolling or sliding on a flat surface. During the test, 400 seeds are initially added to the box or cylinder. Then, the side plate or cylinder is lifted upwards, and the seeds will scatter around and form a seed pile above the bottom trough. The angle between the inclined surface of the seed pile and the horizontal plane is the angle of repose θ. The simulation test of the box side plates lifting method is shown in Figure 11. The simulation test of the cylinder lifting method is shown in Figure 12.

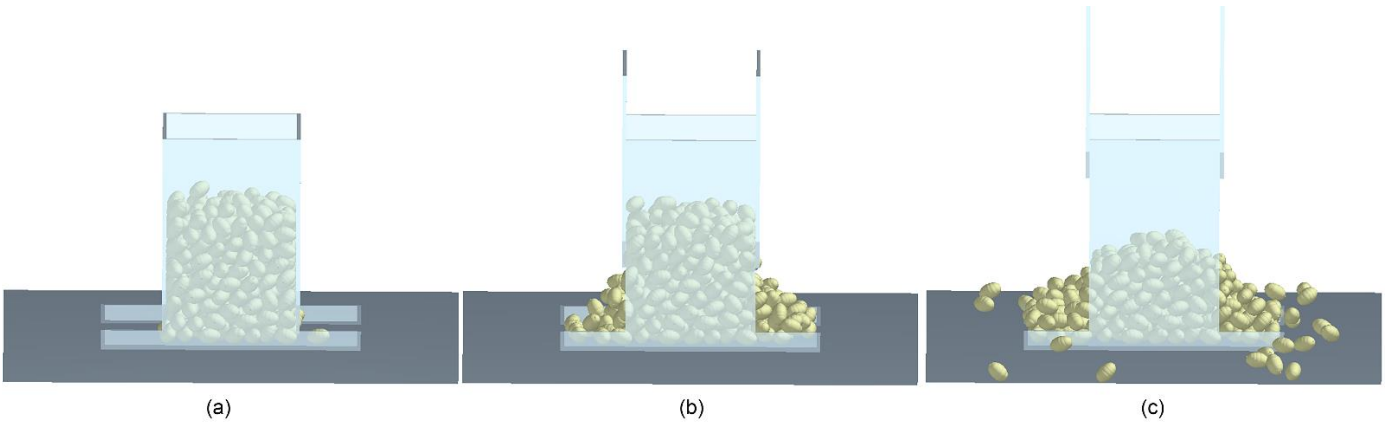

Figure 11. Simulation test of box side plates lifting method. (**a**) initial state, (**b**) side plates lifting, (**c**) test completed.

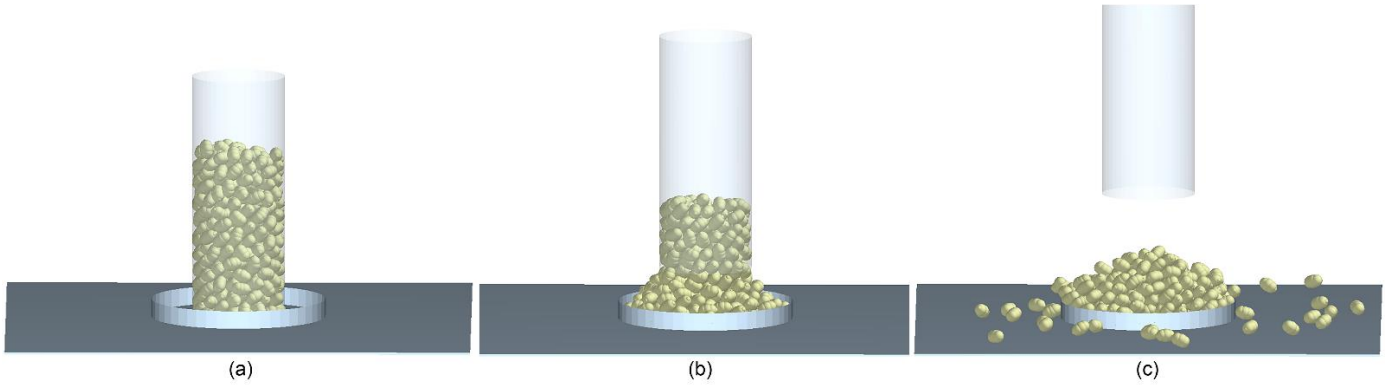

Figure 12. Simulation test of cylinder lifting method. (**a**) initial state, (**b**) cylinder lifting, (**c**) test completed.

Due to the relatively large size of potato minituber seeds, relatively large gaps will be generated between them when they are piled up. Therefore, direct measurement of the angle of repose may bring some errors. In this paper, image processing and angle acquisition of the angle of repose images are conducted, respectively, through Matlab 2019 and Origin 2022 software, as depicted in Figure 13. Firstly, a frontal view of the angle of repose is captured. Subsequently, the captured image of the angle of repose is subjected to grayscale processing and binarization in Matlab software to clarify the boundary contour. Then, dilation processing is performed on the binarized image, and the boundary contour curve is extracted. In Origin software, the coordinates of the boundary curve are extracted, and then the extracted coordinate data are subjected to linear fitting. The tangent of the angle of repose is the slope of the fitted straight line.

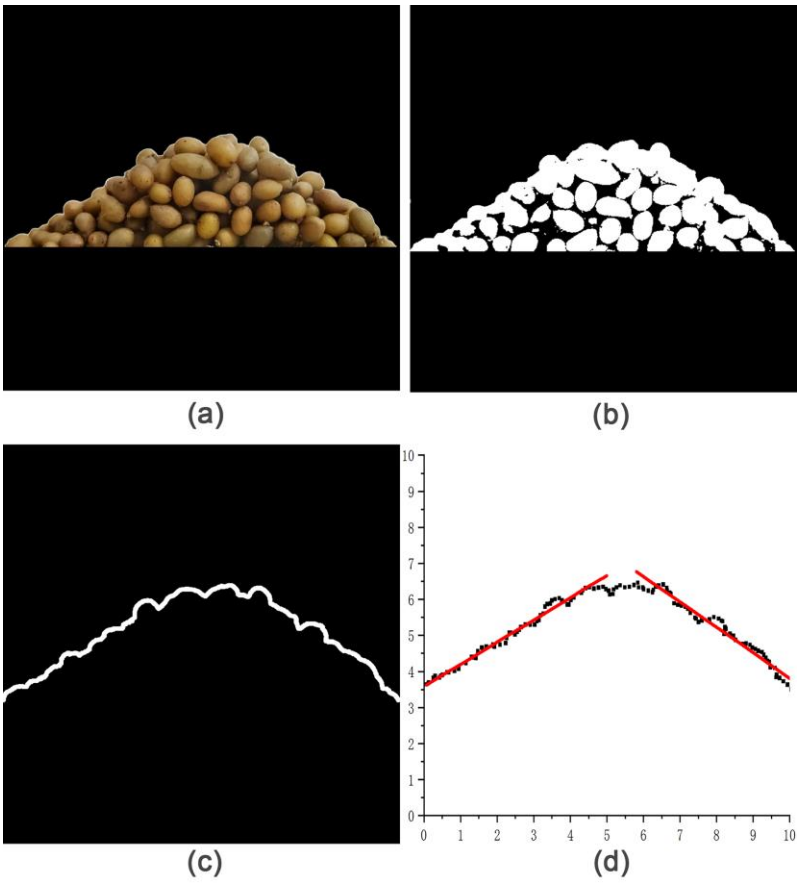

Figure 13. Repose angle image processing and angle acquisition. (**a**) initial image, (**b**) binarization, (**c**) boundary extraction, (**d**) linear fitting.

The values of the repose angle mentioned below are the average values obtained from the two test methods mentioned above. By conducting actual tests five times repetitively, the actual repose angle (θ) was measured to be 28.9°.

2.3.2. Steepest Climb Test

The steepest climb test is employed to determine an optimal value range and intermediate level for subsequent tests. Firstly, simulation tests are conducted under various combinations of seed-to-seed contact parameters. Subsequently, the simulated repose angle (θ') is measured, and the relative error (σ) between θ' and θ is calculated.

Based on experience and the literature [18,32], the seed-to-seed collision recovery coefficient (e_x') for potato minituber seeds ranges approximately from 0.20 to 0.80, the seed-to-seed static friction coefficient (μ_s') approximately from 0.15 to 0.75, and the seed-to-seed rolling friction coefficient (μ_r') approximately from 0.01 to 0.07. A total of 400 seeds were generated in the simulation test, with the ratio of ellipsoidal seeds to spherical seeds being 80% to 20%, respectively. The lifting speeds of both the side plates and the cylinder were set at 0.01 m/s. In the repose angle test, as there is little contact between seeds and the testing device, the main factor influencing the magnitude of the repose angle is the seed-to-seed contact parameters. Based on experience and referring to the relevant literature [32], in the simulation test, the collision recovery coefficient, static friction coefficient, and rolling friction coefficient between seeds and the testing device are set to 0.46, 0.40, and 0.05, respectively. These parameters will also be used in the subsequent verification test. Each group of tests was repeated 5 times. The test plan and simulation results are presented in Table 4.

Table 4. Simulation test of steepest climb.

Test Number	Simulation Test Factor			Result	
	e_x'	μ_s'	μ_r'	θ'/°	σ/%
1	0.20	0.15	0.01	23.1	23.9
2	0.30	0.25	0.02	26.1	20.2
3	0.40	0.35	0.03	27.9	17.5
4	0.50	0.45	0.04	29.4	3.3
5	0.60	0.55	0.05	31.4	9.8
6	0.70	0.65	0.06	34.3	15.5
7	0.80	0.75	0.07	35.8	19.1

It can be known from Table 4 that the σ value decreases first and then increases, with the minimum value of 3.3% in group 4. Hence, group 4 is selected as the intermediate level, and groups 3 and 5 are respectively taken as the low level and the high level for the three-factor and five-level rotational combination test. The optimized ranges of e_x', μ_s', and μ_r' are 0.40 to 0.60, 0.35 to 0.55, and 0.03 to 0.05, respectively.

2.3.3. Quadratic Orthogonal Rotation Combination Design Test

The e_x', μ_s', and μ_r' of the potato minituber seed were selected as test factors, with σ as test index. A three-factor, five-level quadratic orthogonal rotatable combination test was conducted. The five levels for each of the three simulation factors were coded from low to high, as detailed in Table 5; the corresponding experimental designs and results are presented in Table 6. The values of the repose angle in the test results were all the averages of the results measured by the two test methods. In Tables 5–7, "A", "B", and "C" refer to the seed-to-seed collision recovery coefficient, the seed-to-seed static friction coefficient, and the seed-to-seed rolling friction coefficient, respectively.

Table 5. Code of test factors.

Code	Test Factor		
	A	B	C
−1.682	0.40	0.35	0.030
−1	0.45	0.40	0.035
0	0.50	0.45	0.040
1	0.55	0.50	0.045
1.682	0.60	0.55	0.050

Table 6. Test scheme and results.

Test Number	Test Factor			Relative Error σ (%)
	A	B	C	
1	−1	−1	−1	18.2
2	1	−1	−1	15.5
3	−1	1	−1	19.0
4	1	1	−1	14.8
5	−1	−1	1	15.1
6	1	−1	1	14.7
7	−1	1	1	8.5
8	1	1	1	9.8
9	−1.682	0	0	16.2
10	1.682	0	0	15.3
11	0	−1.682	0	20.0
12	0	1.682	0	11.7
13	0	0	−1.682	17.9
14	0	0	1.682	12.9
15	0	0	0	0.8
16	0	0	0	2.6
17	0	0	0	3.9
18	0	0	0	2.0
19	0	0	0	1.1
20	0	0	0	3.2

Table 7. Analysis of variance.

Source of Variance	Sum of Squares	Df	Mean Sum of Squares	F	*p*
model	802.35	9	89.15	30.78	<0.0001 **
A	4.13	1	4.13	1.43	0.2598
B	47.09	1	47.09	16.26	0.0024 **
C	56.63	1	56.63	19.55	0.0013 **
AB	0.0050	1	0.0050	0.0017	0.9677
AC	7.60	1	7.60	2.63	0.1362
BC	16.82	1	16.82	5.81	0.0367 *
A^2	271.30	1	271.30	93.68	<0.0001 **
B^2	275.73	1	275.73	95.21	<0.0001 **
C^2	256.04	1	256.04	88.41	<0.0001 **
Residual	28.96	10	2.90		
Lack of fit	21.73	5	4.35	3.00	0.1263
Error	7.23	5	1.45		
Sum	831.31	19			

Note: * indicates significant ($p \leq 0.05$), ** indicates highly significant ($p \leq 0.01$).

The simulation data underwent regression analysis using Design-Expert 13 software. The significance analysis of these three test factors on the test index is summarized in Table 7. As indicated by Table 7, the B, C, A^2, B^2, and C^2 exert highly significant effects

on the relative error σ of the angle of repose, while interaction term BC also significantly influences this relative error. Conversely, A, along with interaction terms AB and AC, does not demonstrate a significant effect on the test index.

The 3D response surfaces of the three interaction terms AB, AC, and BC are presented in Figure 14. As can be seen from BC, the relative error σ between the simulated and actual repose angles in the simulation tests first decreases and then increases with the increase in B and C. The response surface and contour lines of C within the unit range are steeper and denser than those of B. The steeper the response surface and the denser the contour lines, the more significant the influence of this factor on the result. Therefore, the seed-to-seed rolling friction coefficient has a more significant effect on the accumulation angle than the seed-to-seed static friction coefficient, which is consistent with the results obtained from the analysis of variance.

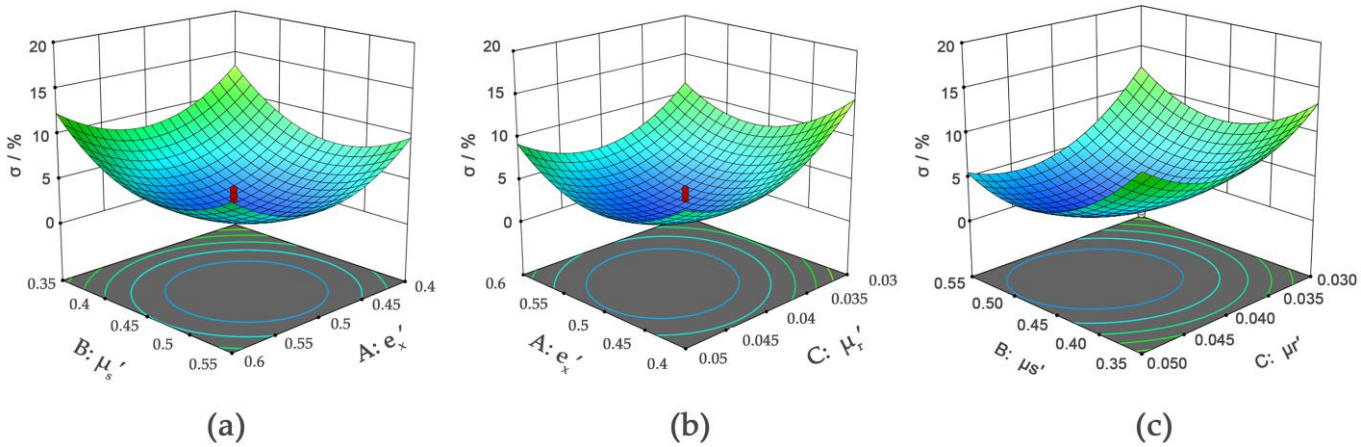

Figure 14. 3D response surface diagram of interaction term BC. (**a**) interaction terms AB, (**b**) interaction terms AC, (**c**) interaction terms BC.

After excluding non-significant terms A, AB, and AC, a new fitting regression equation (expressed in actual values) is derived as follows:

$$\sigma = 136.89 - 315.39B - 2577.79C - 1450BC - 0.91A^2 + 394.24B^2 + 37{,}833.33C^2 \quad (9)$$

The *p*-value of the regression model is less than 0.01; the *p*-value of the residual term is greater than 0.05; the coefficient of determination R^2 = 0.95, indicating that this regression model is highly significant; the reliability of the regression equation is high, and it can accurately reflect the relationship between the three test factors and the relative error of the repose angle.

2.3.4. Parameter Optimization Based on Genetic Algorithm

With the rapid advancement of modern computer science, an increasing number of practical problems require resolution through optimization algorithms. Genetic algorithms represent a class of optimization techniques that simulate the principles of biological evolution to address these challenges. The computational process encompasses several steps, including population initialization, fitness evaluation, selection, crossover, mutation, and iterative optimization. In genetic algorithms, each candidate solution is treated as a chromosome that evolves through genetic operations such as crossover and mutation. During this evolutionary process, unfit chromosomes are eliminated while those with higher fitness are preserved and allowed to reproduce. Consequently, after multiple iterations, the chromosome exhibiting the highest fitness emerges as the sought-after optimal solution.

It is evident from Table 7 that the seed-to-seed collision restitution coefficient (A) is not a significant factor; therefore, it has been assigned an intermediate level. The optimization

objective focuses on minimizing the relative error σ, and Equation (9) is addressed using a genetic algorithm implemented in Matlab. The objective function and constraints are detailed as follows:

According to Table 7, it is evident that the coefficient of seed-to-seed collision recovery (A) is a non-significant factor; therefore, it has been assigned a mid-level value in order to minimize the relative error σ between simulated and actual repose angles as part of our optimization objective. Utilizing Matlab-based genetic algorithms for solving Equation (9) yields the following objective function and constraints:

$$\begin{cases} min\sigma(A,B,C) \\ s.t. \begin{cases} A = 0.5 \\ 0.35 \leq B \leq 0.55 \\ 0.03 \leq C \leq 0.05 \end{cases} \end{cases} \tag{10}$$

The optimal values for the three seed-to-seed contact parameters—e_x, μ_s, and μ_r—are determined to be 0.500, 0.476, and 0.043, respectively. Under this optimal configuration, the relative error achieved is 1.8%.

3. Results and Discussion

3.1. Verification Device and Method

To achieve a more comprehensive validation of the calibrated contact parameters, this study designed a test device that integrates both collision and accumulation, as illustrated in Figure 15. The device primarily consists of an acrylic box, a wide-mouth funnel, a rubber inclined plane, and a rubber flat surface. The dimensions of the acrylic box are 250 mm in length, 70 mm in width, and 330 mm in total height. According to the preliminary test, under this width, only a small number of seeds are needed to form the angle of repose well. Both the top and bottom surfaces remain open, with lower openings on the left and right sides positioned above the rubber flat surface. The rubber inclined plane is affixed to the left side wall of the box, while the wide-mouth funnel is situated directly above it at the opening of the box; its primary function is to control the falling trajectory of seeds so that they can descend vertically and collide with the inclined plane.

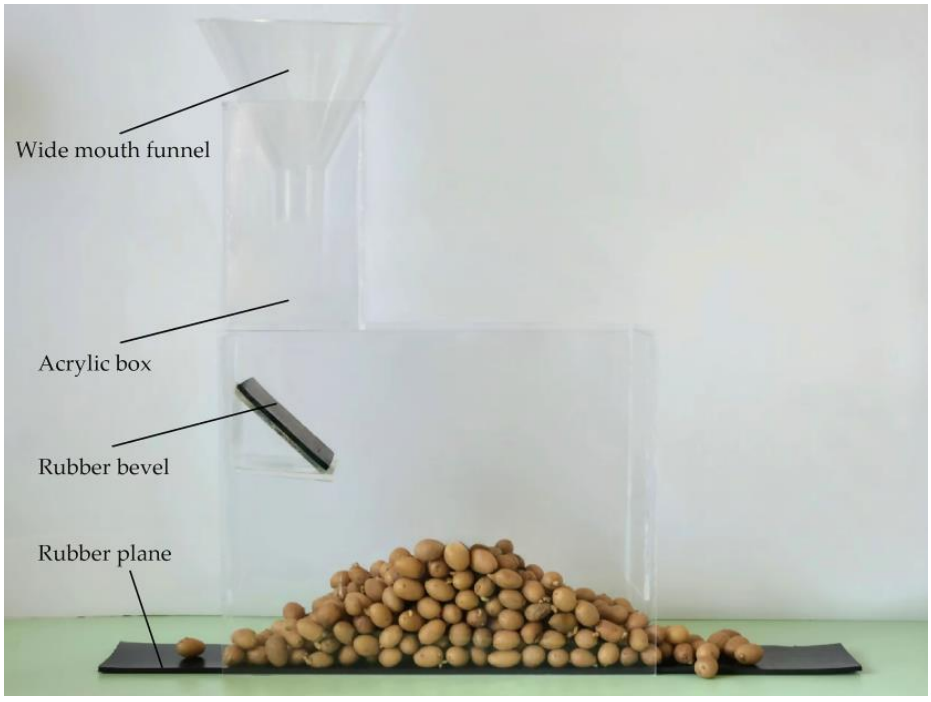

Figure 15. Test verification device physical drawing.

Seeds are released from the funnel outlet and, during their descent, initially collide with the rubber inclined plane below before rebounding to the right and subsequently falling onto the rubber flat surface. As more seeds descend, a seed pile gradually forms. The simulation of this seed descent process is illustrated in Figure 16. The horizontal distance (h) between the centerline of the seed pile and the collision point is primarily influenced by both the initial height of descent and the contact parameters between the seeds and the rubber inclined plane. When maintaining a constant initial descent height, this horizontal distance is predominantly determined by these contact parameters. The repose angle (γ) of the seed pile formed after the seeds drop onto the rubber plane is jointly determined by the contact parameters of seed-to-seed and seed-to-rubber. Therefore, h and γ can be taken as two validation indicators, and the relative errors (δ) between the simulation tests and the actual tests can reflect the accuracy of the calibrated parameters.

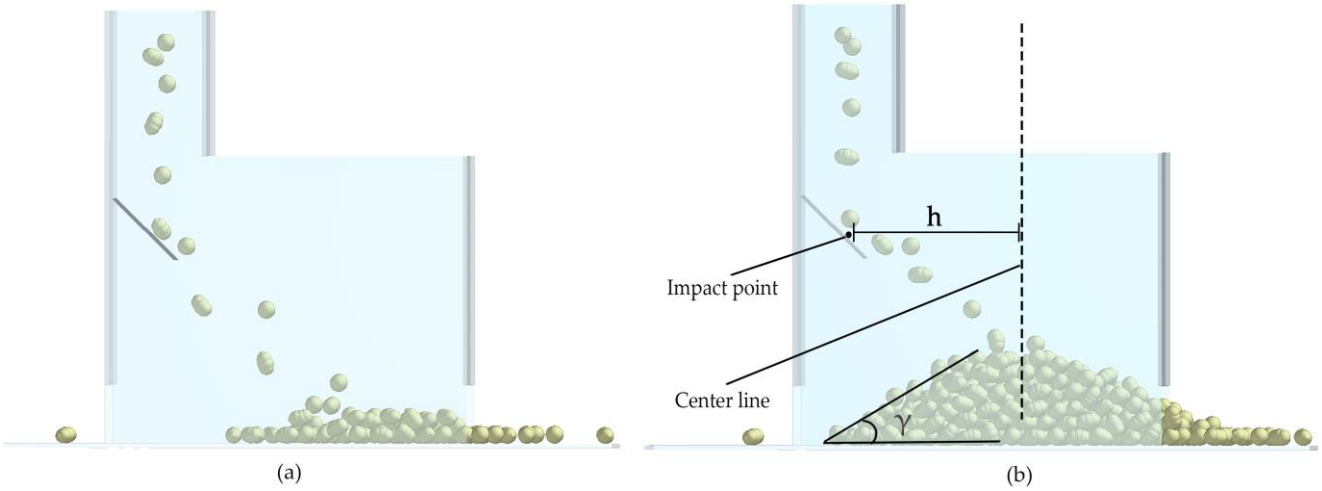

Figure 16. Simulation seed drop test. (**a**) seeds began to pile up, (**b**) seed pile is almost complete.

Neither too large nor too small a rebound distance is desirable. If the rebound distance is too large, the landing points of the seeds will be relatively scattered, and the efficiency of forming the seed pile will be reduced. If the rebound distance is too small, it will also be unfavorable for the formation of the angle of repose and will simultaneously affect the verification effect of the parameters. Based on the results of the preliminary test, we determined parameters such as the height of the funnel outlet and the height of the rubber bevel. The outlet at the base of the funnel was positioned 280 mm above the rubber plane. The length of the rubber bevel is 70 mm, the width is 70 mm, and the angle is 45°. The lower edge of the rubber bevel is located 150 mm above the rubber plane. Seeds were introduced slowly and uniformly into the funnel for the actual tests. Each test was conducted ten times, and results were averaged to ensure reliability. Ultimately, the measured actual repose angle was found to be 30.6°, with a horizontal distance of 123 mm between the centerline of the seed pile and the collision point. The calibrated simulation parameters for potato minituber seeds were subsequently input into EDEM for simulation tests, maintaining consistency with conditions from actual tests. A total of 400 seeds were generated at a rate of 30 seeds per second, with ellipsoidal seeds comprising 80% and spherical seeds making up 20%. The gravity acceleration setting is 9.81 m/s^2. The height and diameter of the virtual plane in the particle factory are kept consistent with the height and diameter of the funnel outlet in the actual test. The Rayleigh step size is set to 20%. These simulation tests were also repeated ten times to obtain average results.

3.2. Verification Results

The test results are shown in Table 8. The final simulated repose angle measured was recorded as 32.1°, along with a horizontal distance of 116 mm between the centerline of the seed pile and its impact point. The relative errors between these two indicators in both

simulation and actual tests were determined to be 4.9% and 5.6%, respectively. The errors are within the acceptable range, which indicates that the calibrated contact parameters described in the paper are relatively accurate.

Table 8. Verification test results.

Test Number	Repose Angle γ (°)	Horizontal Distance h (mm)
1	31.5	113
2	32.6	121
3	32.4	114
4	31.8	116
5	31.7	119
6	32.2	113
7	32.1	120
8	33.0	117
9	31.2	115
10	32.8	112
Average value	32.1	116

Apart from the experimental methods and verification methods, just looking at the results, the most significant difference between the calibration results in this paper and those of other similar studies lies in the rolling friction coefficient between the seeds and the contact materials. The rolling friction coefficient between the seeds and the materials calibrated in this paper is 0.0062, while the calibrated values in other studies are mostly above 0.02. The main reason is that the contact material adopted in this study is rubber, which has a smooth surface, while the contact materials used in other studies are mostly steel plates, whose surfaces are relatively rough. On a rough surface, the protrusions and depressions on its surface will generate more mechanical interlocking when they are in contact with each other. This mechanical interlocking will create additional resistance when the seeds are in motion, thus increasing the coefficient of friction. Therefore, the rolling friction coefficient between the seeds and the contact materials measured in this study is significantly lower than that in other studies. This is also one of the values of this study, that is, it can provide a reference for the discrete element simulation of potato minituber equipment using rubber materials.

In terms of the seed-to-seed contact parameters, the calibrated results in this study seem to be slightly larger than those in other similar studies. The reason may lie in the fact that the triaxial dimensions (length L, width W and thickness T) of the seeds used in this study are smaller than those in other studies.

For the seed-to-seed collision recovery coefficient, the collision between small-sized seeds is closer to point contact, and the interaction time of the collision may be shorter. This enables the seeds to recover their deformation more quickly after the collision, which, to some extent, leads to a larger result than other studies. As for the seed-to-seed static friction coefficient, the smaller seed size means that the seeds may be more likely to embed themselves into the microscopic protrusions and depressions on the contact surface. Due to the closer contact, the coefficient of static friction becomes larger. Regarding the seed-to-seed rolling friction coefficient, because of the small seed size, during the rolling process, the contact area between seeds may be relatively more prone to local adhesion phenomena, resulting in relatively greater resistance during rolling and thus a relatively increased result.

Overall, in our study, the combination of the smaller size of the seeds and the relatively smooth contact surface has led to certain differences between the parameters we calibrated and those in other studies.

4. Conclusions

The intrinsic parameters including the three-axis dimensions, density, elastic modulus, and Poisson's ratio of V7 potato minituber seeds were acquired via physical test, and the discrete element model of the seeds was constructed. By conducting three mechanical tests

and using a methodology that combines simulation tests with actual tests, the collision recovery coefficient, static friction coefficient, and rolling friction coefficient between seeds and rubber materials were determined to be 0.469, 0.474, and 0.0062, respectively. The calibration of the three seed-to-seed contact parameters was performed concurrently through a repose angle test that combines the box side plates lifting method with the cylinder lifting method, in conjunction with response surface methodology. The regression equation underwent optimization using a genetic algorithm implemented in Matlab, ultimately yielding an optimal combination of seed-to-seed simulation contact parameters: specifically, the seed-to-seed collision recovery coefficient, static friction coefficient, and rolling friction coefficient were found to be 0.500, 0.476, and 0.043.

The accuracy of the calibration results was verified by a combination of collision and accumulation seed drop verification test. The relative errors of the two verification indicators in the simulation and actual tests were 4.9% and 5.6%, respectively, with small errors. The verification results show that the parameter calibration method proposed in this paper is feasible and the calibration results are also reliable.

Due to the thin skin of the potato minituber, which is prone to damage, and considering that rubber materials are softer and smoother than the commonly used steel plate materials, the seed planter with rubber materials as the contact surfaces can achieve low-damage seed-metering in a better way. The calibration results of this paper can provide a reference and theoretical basis for the selection of simulation contact parameters in the discrete element simulation analysis of the potato minituber seed planter and further offer help for the design and optimization of their structures.

Author Contributions: Conceptualization, W.M.; methodology, K.C. and X.Y.; software, K.C.; validation, C.J. and X.Y.; formal analysis, Y.L. and C.J.; investigation, Y.L.; resources, W.M.; data curation, X.Y.; writing—original draft preparation, K.C.; writing—review and editing, K.C. and X.Y.; visualization, C.J.; supervision, W.M.; project administration, W.M.; funding acquisition, W.M. All authors have read and agreed to the published version of the manuscript.

Funding: This research was funded by the Pilot Project for the Integration of Agricultural Machinery R & D, Manufacturing, Promotion and Application in Shandong Province (Grant No. NJYTHSD-202308), the National Key Research and Development Program of China (Grant No. 2021YFD2000502), and the National Natural Science Foundation of China (Grant No. 32171910).

Institutional Review Board Statement: Not applicable.

Data Availability Statement: Data are contained within the article.

Acknowledgments: The author is grateful to the reviewers and the editor for their valuable suggestions and assistance, as well as to the fund for providing financial support.

Conflicts of Interest: All authors have no conflicts of interest and agree to publish.

References

1. Yuan, Y. Research on Potato Cultivation Techniques and Promotion. *Agric. Dev. Equip.* **2021**, *12*, 207–208.
2. Pang, S.; Fang, G.; Zhang, X. Application and Development Thoughts of Potato Virus-free Seed Potatoes. *Kexue Zhongyang* **2018**, *12*, 17–19. [CrossRef]
3. Ding, L.; Yang, L.; Wu, D.; Li, D.; Zhang, D.; Liu, S. Simulation and Experiment of Corn Air Suction Seed Metering Device Based on DEM-CFD Coupling Method. *Trans. Chin. Soc. Agric. Mach.* **2018**, *49*, 48–57. [CrossRef]
4. Wang, J.; Tang, H.; Wang, Q.; Zhou, W.; Yang, W.; Shen, H. Numerical simulation and experiment on seeding performance of pickup finger precision seed-metering device based on EDEM. *Trans. Chin. Soc. Agric. Eng.* **2015**, *31*, 43–50.
5. Ling, J.; Gu, M.; Luo, W.; Shen, H.; Hu, Z.; Gu, F.; Wu, F.; Zhang, P.; Xu, H. Simulation Analysis and Test of a Cleaning Device for a Fresh-Peanut-Picking Combine Harvester Based on Computational Fluid Dynamics–Discrete Element Method Coupling. *Agriculture* **2024**, *14*, 1594. [CrossRef]
6. Xing, W.; Zhang, H.; Sun, W.; Li, H.; Liu, X.; Li, H.; Chen, Y.; Lu, Y. Performance Study of a Chain–Spoon Seed Potato Discharger Based on DEM-MBD Coupling. *Agriculture* **2024**, *14*, 1520. [CrossRef]
7. Zheng, X.; He, X.; Shang, S.; Wang, D.; Li, C.; Shi, Y.; Zhao, Z.; Lu, Y. Calibration and Experiments for Discrete Element Simulation Parameters of Cyperus Esculentus Seeds. *J. Agric. Mech. Res.* **2024**, *46*, 172–178.

8. Chen, J.; Jiang, P.; Liu, J.; Zhang, X.; Shi, Y. Calibration and Modeling of Parameters for Kale Root Stubble Simulation Based on the Discrete Unit Method. *Agronomy* **2023**, *13*, 2298. [CrossRef]
9. Ma, X.; You, Y.; Yang, D.; Wang, D.; Hui, Y.; Li, D.; Wu, H. Calibration and Verification of Discrete Element Parameters of Surface Soil in Camellia Oleifera Forest. *Agronomy* **2024**, *14*, 1011. [CrossRef]
10. Li, M.; He, X.; Zhu, G.; Liu, J.; Gou, K.; Wang, X. Modeling and Parameter Calibration of Morchella Seed Based on Discrete Element Method. *Appl. Sci.* **2024**, *14*, 11134. [CrossRef]
11. Dai, Z.; Wu, M.; Fang, Z.; Qu, Y. Calibration and Verification Test of Lily Bulb Simulation Parameters Based on Discrete Element Method. *Appl. Sci.* **2021**, *11*, 10749. [CrossRef]
12. Rao, G.; Zhao, W.; Shi, L.; Sun, B.; Guo, J.; Wang, Z. Calibration and experimental validation of discrete element simulation parameters for double-low rapeseed. *J. China Agric. Univ.* **2023**, *28*, 192–207. [CrossRef]
13. Li, Z.; Liu, F.; Wei, Z.; Deng, C.; Wang, S.; Xie, S. Parameter calibration of discrete element model of stem mustard seeds. *J. Chin. Agric. Mech.* **2023**, *44*, 83–90. [CrossRef]
14. Jin, X.; Zhang, J.; Xue, J.; Guo, C.; He, C.; Lu, L. Calibration of Discrete Element Contact Parameters of Maize Seed and Rubber Belt. *J. Agric. Mech. Res.* **2022**, *44*, 39–43. [CrossRef]
15. Zhang, S.; Zhang, R.; Chen, T.; Fu, J.; Yuan, H. Calibration of simulation parameters of mung bean seeds using diserete element method and verification of seed-metering test. *Trans. Chin. Soc. Agric. Mach.* **2022**, *53*, 71–79.
16. Chen, Y.; Gao, X.; Jin, X.; Ma, X.; Hu, B.; Zhang, X. Calibration and Analysis of Seeding Parameters of Cyperus Esculentus Seeds Based on Discrete Element Simulation. *Trans. Chin. Soc. Agric. Mach.* **2023**, *54*, 58–69.
17. Ji, J.; Yu, L.; Wu, X.; Su, W.; Xiao, Y.; Zhang, Z. Parameter Calibration of Discrete Element Simulation of Sorghum Seed for Wine Use. *J. Agric. Mech. Res.* **2024**, *46*, 46–52.
18. Liu, W.; He, J.; Li, H.; Li, X.; Zheng, K.; Wei, Z. Calibration of Simulation Parameters for Potato Minituber Based on EDEM. *Trans. Chin. Soc. Agric. Mach.* **2018**, *49*, 125–135+142.
19. Ding, X.; Li, K.; Hao, W.; Yang, Q.; Yan, F.; Cui, Y. Calibration of Simulation Parameters of Camellia oleifera Seeds Based on RSM and GA-BP-GA Optimization. *Trans. Chin. Soc. Agric. Mach.* **2023**, *54*, 139–150. [CrossRef]
20. Li, G.; Ma, J.; Tian, X.; Zhao, C.; An, S.; Guo, R.; Feng, B.; Zhang, J. Discrete Meta-Simulation of Silage Based on RSM and GA-BP-GA Optimization Parameter Calibration. *Processes* **2023**, *11*, 2784. [CrossRef]
21. Niu, Z.; Sun, Z.; Chen, C.; Shi, Y.; Zhao, C. Optimization of the Rotor Structure of a Hollow Traveling Wave Ultrasonic Motor Based on Response Surface Methodology and Self-adaptive Genetic Algorithm. *Proc. CSEE* **2014**, *34*, 5378–5385.
22. Zhao, J.; Liu, F.; Xia, L.; Fan, Y. Passive shimming optimization method of MRI based on genetic algorithm-sequential quadratic programming. *J. Zhejiang Univ. Eng. Sci.* **2024**, *58*, 1305–1314.
23. Tang, H.; Xu, W. Resource optimized scheduling based on improved genetic algorithm. *Mod. Electron. Tech.* **2024**, *47*, 169–172. [CrossRef]
24. Liu, R.; Li, Y.; Liu, Z.; Liu, L.; Lu, H. Analysis and calibration of discrete element parameters of coated maize seed. *Trans. Chin. Soc. Agric. Mach.* **2021**, *52*, 1–8+18.
25. Chen, S.; Jiang, L.; Lin, X.; Tang, X.; Liu, X.; Zhang, L. Calibration tests for the contact parameters of flour particle based on discrete element method. *Trans. Chin. Soc. Agric. Eng.* **2024**, *40*, 8. [CrossRef]
26. Liu, D.; Duan, J.; Chen, X.; Xiong, Z.; Wang, X.; Xie, F. Calibration of Friction Parameters of Seed Particle Models of Hybrid Rice Based on EDEM. *J. Shenyang Agric. Univ.* **2023**, *54*, 189–195. [CrossRef]
27. Bai, S.; Yuan, Y.; Niu, K.; Zhou, L.; Zhao, B.; Wei, L.; Liu, L.; Xiong, S.; Shi, Z.; Ma, Y.; et al. Simulation Parameter Calibration and Experimental Study of a Discrete Element Model of Cotton Precision Seed Metering. *Agriculture* **2022**, *12*, 870. [CrossRef]
28. Li, D.; Wang, R.; Zhu, Y.; Chen, J.; Zhang, G.; Wu, C. Calibration of Simulation Parameters for Fresh Tea Leaves Based on the Discrete Element Method. *Agriculture* **2024**, *14*, 148. [CrossRef]
29. Chen, X.; Bai, J.; Wang, X.; Fang, W.; Hong, T.; Zang, N.; Fang, L.; Wang, G. Calibration and Testing of Discrete Elemental Simulation Parameters for Pod Pepper Seeds. *Agriculture* **2024**, *14*, 831. [CrossRef]
30. Wen, Y.; Liu, M.; Liu, R.; Liu, B.; Shao, Y. Comparative Study Between Numerical Simulation by Discrete Element Method and Typical Experimental Research of Particles. *China Powder Sci. Technol.* **2015**, *21*, 1–5. [CrossRef]
31. Ma, S.; Xu, L.; Xing, J.; Yuan, Q.; Duan, Z.; Yu, C.; Chen, C. Study on collision damage experiment of grape and finite element analysis. *J. China Agric. Univ.* **2018**, *23*, 180–186.
32. Yu, C.; Duan, H.; Cai, X.; Xu, T.; Yao, F.; Chen, Z.; Yan, F. Discrete element simulation parameters-based measurement of materials for potato minituber. *J. Huazhong Agric. Univ.* **2021**, *40*, 210–217. [CrossRef]